Vol 16 No 6, June 2007
1009-1963/2007/16(06)/1665-07
Chinese Physics
© 2007 Chin. Phys. Soc.
and IOP Publishing Ltd

Diffractive characteristics of the liquid crystal spatial light modulator*

Cao Zhao-Liang(曹召良)[a)b)†], Mu Quan-Quan(穆全全)[a)b)],
Hu Li-Fa(胡立发)[a)], Liu Yong-Gang(刘永刚)[a)], and Xuan Li(宣 丽)[a)]

[a)] *State Key Laboratory of Applied Optics, Changchun Institute of Optics, Fine Mechanics and Physics, Chinese Academy of Sciences, Changchun* 130033, *China*
[b)] *Graduate School of the Chinese Academy of Sciences, Beijing* 100039, *China*

(Received 9 October 2006; revised manuscript received 7 November 2006)

The liquid crystal spatial light modulator (LC SLM) is very suitable for wavefront correction and optical testing and can produce a wavefront with large phase change and high accuracy. The LC SLM is composed of thousands of pixels and the pixel size and shape have effects on the diffractive characteristics of the LC SLM. This paper investigates the pixel effect on the phase of the wavefront with the scalar diffractive theory. The results show that the maximum optical path difference modulation is 41 μm to produce the paraboloid wavefront with the peak to valley accuracy better than $\lambda/10$. Effects of the mismatch between the pixel and the period, and black matrix on the diffraction efficiency of the LC SLM are also analysed with the Fresnel phase lens model. The ability of the LC SLM is discussed for optical testing and wavefront correction based on the calculated results. It shows that the LC SLM can be used as a wavefront corrector and a compensator.

Keywords: liquid crystal spatial light modulator, diffraction efficiency, pixel, wavefront
PACC: 4225F, 4210D

1. Introduction

The liquid crystal spatial light modulator (LC SLM) is very suitable for wavefront correction, optical testing and phase filter[1] and it has been investigated in many papers.[2−9] In these applications, the large phase modulation should be produced with the kinoform technique.[10−12] The remainder after the wavefront modulo 2π should be quantified by multilevel step. As the pixel has certain size and shape, the remainder is discretized and piecewise approximated by it. Thus, the quantified and discretized wavefront deviates from the ideal wavefront and the diffraction efficiency is also decreased. We should quantificationally calculate the effect of the pixel on the wavefront deviation and diffraction efficiency in order to obtain the accurate wavefront and high diffraction efficiency.

Many papers have investigated the diffraction efficiency. Different methods are given about how to obtain the high diffraction efficiency of the Fresnel lens encoded in low resolution devices.[13−15] In this paper, we mainly consider the situation that one period does not include the integer number of the pixel. In other words, one pixel which is located at the interface of two periods is possible to be divided to two parts and we call it mismatch between the period and the pixel. Thus, it will affect the diffraction efficiency and we will discuss this effect. The effect of the black matrix on the diffraction efficiency is also discussed.

While the LC SLM is used as a tunable Fresnel lens, the diffraction efficiency is very important. However, the phase distribution should be specially attended if it is utilized for optical testing and wavefront correction. We must discuss the effect of low spatial resolution on the phase of the wavefront. As far as we know, no one has analysed the wavefront deviation error caused by the pixel. We mainly discuss the effects of the quantization and discretization caused by the pixel on the phase of the wavefront in Sec.2. A LC SLM with 2 cm × 1.5 cm area, 1024 × 768 pixels, and 19 μm pixel size is utilized as an example in the paper. Ordinarily, if peak to valley (PV) accuracy of the corrected wavefront and the fabricated optical surface is down to $\lambda/10$, the corrected result and the optical surface are good. Therefore, we use $\lambda/10$ as a standard to evaluate the ability of the LC SLM.

*Project supported by the National Natural Science Foundation of China (Nos 60578035, 50473040) and the Science Foundation of Jilin Province (Nos 20050520, 20050321-2).
†E-mail: caozlok@yahoo.com.cn

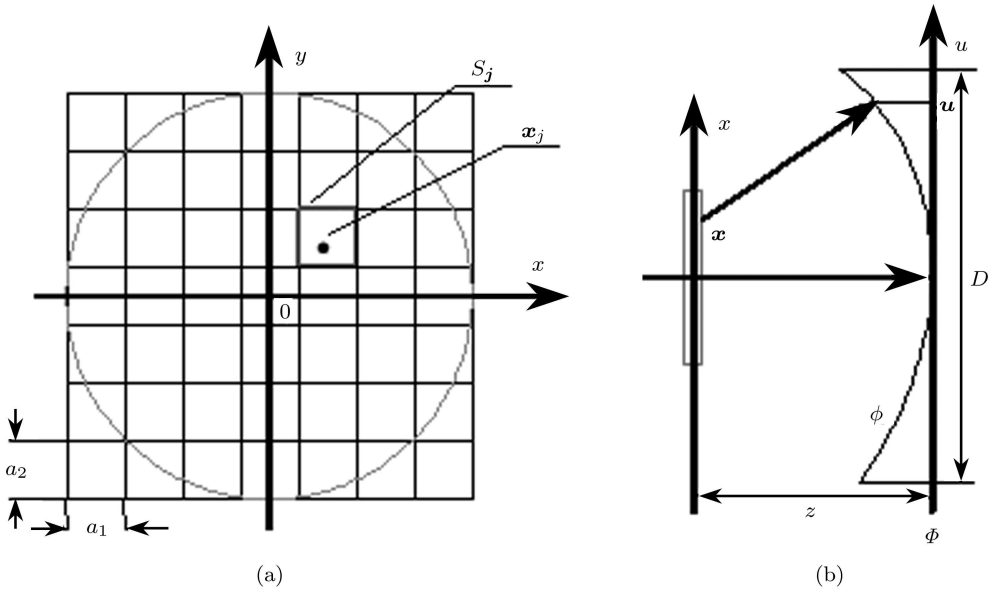
2. Pixel effects on the phase of the wavefront

2.1. Theory

Using the kinoform method to obtain smooth phase functions such as Fresnel phase lens and aspheric, we can write the transfer function as

$$F(\boldsymbol{x}) = \exp[\mathrm{i}\ \mathrm{mod}_{2\pi}\varphi(\boldsymbol{x})], \tag{1}$$

where φ is the smooth phase function, $\mathrm{mod}_{2\pi}\ (\varphi)$ is the value of φ modulo 2π, $\boldsymbol{x} = (x, y)$ are the two dimensional coordinates in the LC SLM plane.



(a) (b)

Fig.1. (a) The field of the LC SLM, the circle represents the area used to produce the wavefront. (b) The wavefront at the distance z from the LC SLM.

As shown in Fig.1(a), the area of the LC SLM can be expressed by

$$S = \bigcup_{\boldsymbol{j}\in J} S_{\boldsymbol{j}},\ S_{\boldsymbol{j}} \cap S_{\boldsymbol{j}'} = 0 \quad \text{if} \quad \boldsymbol{j} \neq \boldsymbol{j}', \tag{2}$$

where $S_{\boldsymbol{j}}$ is the area of one pixel and $\boldsymbol{j} = (j_1, j_2)$ from J set. The discretized and quantized transfer function is given by:

$$\hat{F}(\boldsymbol{x}) = \sum_{\boldsymbol{j}\in J} \exp(\mathrm{i}\hat{\varphi}_{\boldsymbol{j}})\delta_{\boldsymbol{j}}(\boldsymbol{x}). \tag{3}$$

Here $\hat{\varphi}_{\boldsymbol{j}}$ can be achieved by quantify $\varphi_{\boldsymbol{j}}$ to N levels from 0 to 2π with the step $h = 2\pi/N$, $\delta_{\boldsymbol{j}}(\boldsymbol{x})$ is the spot function and is defined as:

$$\delta_{\boldsymbol{j}}(\boldsymbol{x}_{\boldsymbol{j}}) = 1;\quad \delta_{\boldsymbol{j}}(\boldsymbol{x}) = 0 \quad \text{if} \quad \boldsymbol{x} \notin S_{\boldsymbol{j}}. \tag{4}$$

The smooth function satisfies the condition

$$|\boldsymbol{a}\cdot\nabla\varphi| \ll 2\pi; \quad 2\pi/N \ll 2\pi. \tag{5}$$

Where $\nabla = \left(\dfrac{\partial}{\partial x}, \dfrac{\partial}{\partial y}\right)$, $\boldsymbol{a} = (a_1, a_2)$. Thus φ may be expanded in a power series of $(\boldsymbol{x} - \boldsymbol{x}_{\boldsymbol{j}})$:[16]

$$\varphi(\boldsymbol{x}) = \varphi(\boldsymbol{x}_{\boldsymbol{j}}) + (\boldsymbol{x} - \boldsymbol{x}_{\boldsymbol{j}})\nabla\varphi(\boldsymbol{x}_{\boldsymbol{j}}). \tag{6}$$

The quantization noise is:

$$q_{\boldsymbol{j}} = \hat{\varphi}_{\boldsymbol{j}} - \varphi(\boldsymbol{x}_{\boldsymbol{j}}), \quad |q_{\boldsymbol{j}}| \leq h/2. \tag{7}$$

The phase produced by the LC SLM can be expressed as

$$\hat{\varphi}_{\boldsymbol{j}} = \varphi(\boldsymbol{x}) + \Delta\varphi_{\boldsymbol{j}}(\boldsymbol{x}), \quad \boldsymbol{x} \in S_{\boldsymbol{j}}. \tag{8}$$

Here $\Delta\varphi_{\boldsymbol{j}}(\boldsymbol{x}) = q_{\boldsymbol{j}} - (\boldsymbol{x} - \boldsymbol{x}_{\boldsymbol{j}})\nabla\varphi(\boldsymbol{x}_{\boldsymbol{j}})$. The mean squared value of phase error caused by discretization and quantization on the LC SLM plane:[16]

$$\begin{aligned}\Delta\varphi &= \left(< \frac{1}{S}\int_S |\hat{\varphi}(\boldsymbol{x}) - \varphi(\boldsymbol{x})|^2 \mathrm{d}^2\boldsymbol{x} >\right)^{1/2} \\ &= \left\{\frac{1}{3}\left(\frac{\pi}{N}\right)^2 + \frac{1}{12S}\int_S [\boldsymbol{a}\cdot\nabla\varphi(\boldsymbol{x})]^2 \mathrm{d}^2\boldsymbol{x}\right\}^{1/2}.\end{aligned} \tag{9}$$

If the LC SLM is illuminated with the light:

$$E(x) = A_0(\boldsymbol{x})\exp[\mathrm{i}k\,\Psi(\boldsymbol{x})],\ k = \frac{2\pi}{\lambda}. \tag{10}$$

The mean phase error in the plane Φ at a distance $z (z \gg \lambda)$ (Fig.1(b)) from the LC SLM can be evaluated by the Kirchhoff–Sommerfeld integral and it can

be written as[16]

$$\Delta\varphi = \left\{\frac{1}{3}\left(\frac{\pi}{N}\right)^2 + \frac{1}{12}\int_S [\boldsymbol{a}\cdot\nabla\varphi(\boldsymbol{x})]^2\rho(\boldsymbol{x})\mathrm{d}^2\boldsymbol{x}\right\}^{1/2}. \tag{11}$$

Where $\rho(\boldsymbol{x})$ is the normalized intensity distribution of the illuminating light. The mean deviation of the wavefront can be evaluated as

$$\begin{aligned}\Delta w = & \left\{\frac{1}{3}\left(\frac{\lambda}{2N}\right)^2 + \frac{1}{12}\int_S \left[\boldsymbol{a}\cdot\nabla\frac{\varphi(\boldsymbol{x})}{k}\right]^2\rho(\boldsymbol{x})\mathrm{d}^2\boldsymbol{x}\right\}^{1/2} \\ = & \left\{\frac{1}{3}\left(\frac{\lambda}{2N}\right)^2 + \frac{1}{12}\int_S \left[\frac{\boldsymbol{a}\cdot\nabla f(\boldsymbol{u})}{\sqrt{1+|\nabla f(\boldsymbol{u})|^2}} + \boldsymbol{a}\cdot\nabla\,\Psi(\boldsymbol{u}+[z+f(\boldsymbol{u})]\nabla f(\boldsymbol{u}))\right]^2\rho_\phi(\boldsymbol{u})\mathrm{d}^2\boldsymbol{u}\right\}^{1/2}. \end{aligned} \tag{12}$$

Here $f(\boldsymbol{u})$ is the smooth function at $\boldsymbol{u}(u,v)$ coordinates, $\rho_\phi(\boldsymbol{u})$ is the normalized intensity distribution along the wavefront ϕ. If the wavefront ϕ is the surface with rotational symmetry $f(r)(r=|\boldsymbol{u}|)$ and $a_1 = a_2 = a$, the mean deviation of the wavefront Δw can be rewritten as[16]

$$\begin{aligned}\Delta w = & \left\{\frac{1}{3}\left(\frac{\lambda}{2N}\right)^2 + \frac{\pi a^2}{12}\int_0^{D/2}\left[\frac{f'(r)}{\sqrt{1+|f'(r)|^2}}\right.\right. \\ & \left.\left. + \Psi'(r+[z+f(r)]f'(r))\right]^2\rho_\phi(r)r\mathrm{d}r\right\}^{1/2}. \end{aligned} \tag{13}$$

For second order rotational surface:

$$r^2 = 2Rf(r) - (1-e^2)f^2(r). \tag{14}$$

Illuminating with the plane wave of unit amplitude, we get the mean deviation of the wavefront:[16]

$$\begin{aligned}\Delta w = & \left\{\frac{1}{3}\left(\frac{\lambda}{2N}\right)^2 + \frac{a^2}{12e^2}\left[1\right.\right. \\ & \left.\left. - \frac{4R^2}{e^2D^2}\ln\left(1+\frac{e^2D^2}{4R^2}\right)\right]\right\}^{1/2}, \end{aligned} \tag{15}$$

where R is the base curvature at the vertex, e is the eccentricity and $0 < e^2 < 1$ for ellipsoid, $e^2 = 1$ for paraboloid and $e^2 > 1$ for hyperboloid, and D is the aperture diameter of the wavefront ϕ. The first term is produced by the quantization and the second represents the wavefront deviation caused by the discretization.

2.2. Pixel effects on the phase of the wavefront

For convenience, $\mathrm{OPD_L}$ is defined as the OPD (optical path difference) modulation at the LC SLM plane. The OPD modulation of the wavefront ϕ as shown in Fig.1(b) can be calculated by the equation

$$\mathrm{OPD_W} = \mathrm{OPD_L} \times D_\mathrm{W}/D_\mathrm{L}, \tag{16}$$

where D_W and D_L are the diameter of the wavefront ϕ and the LC SLM respectively. According to Eq.(15), R^2/D^2 should be known in order to calculate the wavefront deviation Δw. $\mathrm{OPD_W}$ can be calculated with the known R^2/D^2. Then, $\mathrm{OPD_L}$ can be calculated from Eq.(16). Consequently, we do not give R^2/D^2 directly but use $\mathrm{OPD_L}$ and $\mathrm{OPD_W}$ to represent it.

We have investigated the maximum phase modulation of the LC SLM for optical testing[5] and assumed that only two pixels are used to realize 2π rad phase change at the edge. The first term of Eq.(15) shows that the quantified level N affects the phase of the wavefront as shown in Fig.2. It indicates that 4 levels is necessary to quantify the edge of the wavefront in order to acquire the accuracy (PV) better than $\lambda/10$ ($\lambda = 632.8\,\mathrm{nm}$) and we use 4 quantified levels in the following analysis. Figure 3 indicates that the wavefront deviation keeps constant while e^2 increases. So, we choose the paraboloid ($e^2 = 1$) as an example to analyse the pixel effects on the wavefront.

Figure 4 shows the wavefront deviation as a function of the $\mathrm{OPD_L}$ ($19\,\mu\mathrm{m}$ pixel size and the area is $225\,\mathrm{mm}^2$). It indicates that the maximum $\mathrm{OPD_L}$ is $41\,\mu\mathrm{m}$ for the purpose of obtaining the PV of the wavefront better than $\lambda/10$. The effect of the pixel size on

the wavefront is shown in Fig.5 on the condition that the OPD_L is 41 μm. Now, the minimum pixel size of the LC SLM can be down to 9 μm. For this condition, the accuracy of the wavefront is $\lambda/13$ for 41 μm OPD_L.

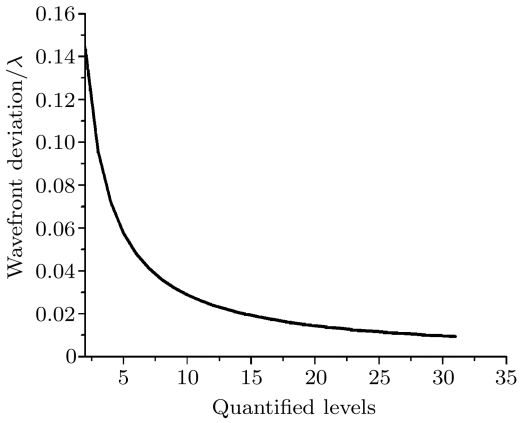


Fig.2. The wavefront deviation as a function of the quantified level.

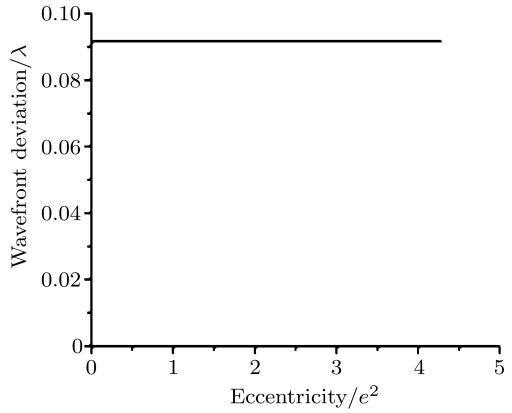


Fig.3. The wavefront deviation as a function of the eccentricity.

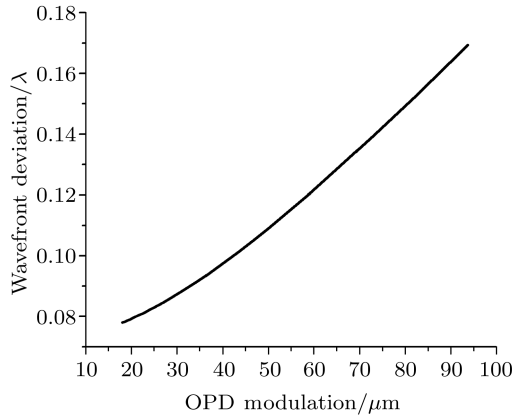


Fig.4. The wavefront deviation as a function of the OPD_L.

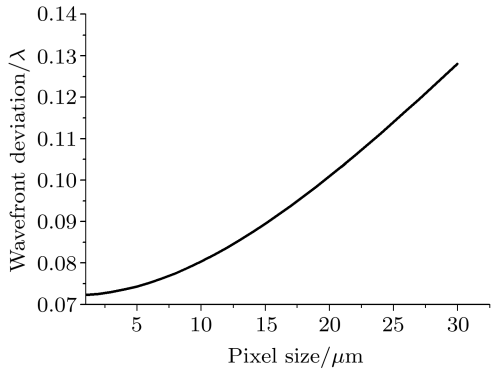


Fig.5. The wavefront deviation as a function of the pixel size, OPD_L is 41 μm.

3. Decrease of the diffraction efficiency caused by the pixel

3.1. Review of the theory

In order to analyse the decrease of the diffraction efficiency, a Fresnel phase lens is used as a model because the wavefront produced by the LC SLM for wavefront correction and optical testing is similar to the sphere wavefront produced by the Fresnel phase lens. According to the rotational symmetry and the periodicity along the r^2 direction, when the Fresnel phase lens is illuminated with a plane wave of unit amplitude, the complex amplitude of the light can be expressed as:[17]

$$f(r^2) = f(r^2 + jr_p^2), \tag{17}$$

where j is an integer and the period is r_p^2. It can be expressed by the Fourier series:

$$f(r^2) = \sum_{n=-\infty}^{+\infty} A_n \exp[\mathrm{i}2\pi n r^2/r_p^2]. \tag{18}$$

The distribution of the complex amplitude at the diffraction order n can be obtained:[18]

$$A_n = 1/r_p^2 \int_0^{r_p^2} f(r^2) \exp[\mathrm{i}2\pi n r^2/r_p^2] \mathrm{d}r^2. \tag{19}$$

For the Fresnel phase lens, the light is mainly concentrated on the first order ($n = 1$). The diffraction efficiency of the Fresnel lens is defined as the intensity of the first order at its primary focus:

$$\eta = I(n = 1) = |A_1|^2. \tag{20}$$

If we can achieve the phase distribution function $f(r^2)$ of the Fresnel lens, the diffraction efficiency can be calculated by Eqs.(19) and (20).

3.2. Mismatch between the pixel and the period

The pixel effects on the diffraction efficiency of the LC SLM are caused by quantification, mismatch between the period and the pixel and black matrix. The effect of the quantification is similar to Fresnel lens fabricated with lithography technique and has been investigated in many papers. In this section, we mainly discuss the mismatch between the period and the pixel. The effect of the black matrix will be analysed in the next section.

Because the pixel has certain size P, the period T cannot be exactly divided by the pixel as shown in Fig.6. This error is similar to the linewidth error caused by the lithography technique. For one period, the integer is n and the remainder is γ after T modulo P. If $\gamma \leq 0.5\,P$, there are n pixels in one period, on the contrary, $n+1$ pixels. So, the maximum error is $0.5\,P$ for the first period. According to Eq.(19), the distribution of the complex amplitude of the first order can be acquired with the known phase distribution function in one period. Then, the diffraction efficiency can be obtained. As shown in Fig.7, when the error of the first period changes from 0 to $0.5\,P$, the diffraction efficiency decreases from 81% to 78.3%. Pixel number effect on the variation of the diffraction efficiency is also calculated while the error is 0.5 P (Fig.8). The decrease of the diffraction efficiency is 1% when the pixel number is 7. So, if the pixel number is not less than 7 in one period, the effect of the pixel size can be ignored.

For 19 μm pixel size and 1024×768 pixels, the diffraction efficiency as a function of the $\mathrm{OPD_L}$ is calculated as shown in Fig.9. It indicates that the diffraction efficiency reduces 30% while the LC SLM is used to correct or produce 41 μm $\mathrm{OPD_L}$. For 9 μm pixel size, the decrease of the diffraction efficiency reduces to 9.5% accordingly.

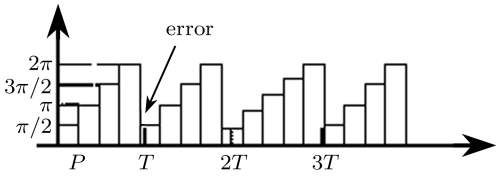


Fig.6. Fresnel phase lens quantified by the pixel.

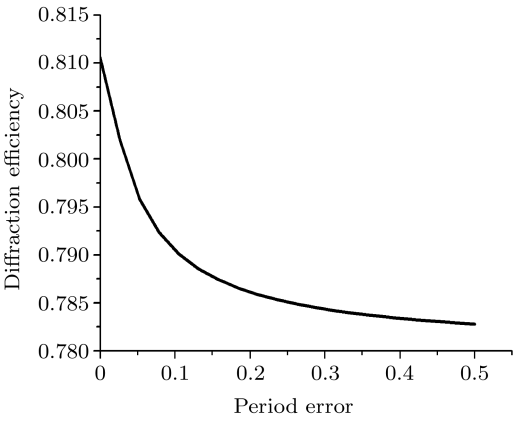


Fig.7. The diffraction efficiency as a function of the period error.

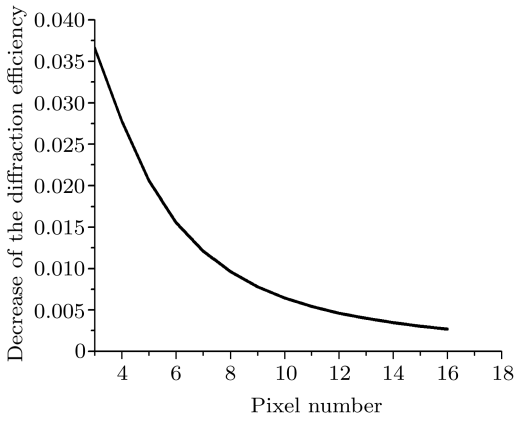


Fig.8. The decrease of the diffraction efficiency as a function of the pixel number.

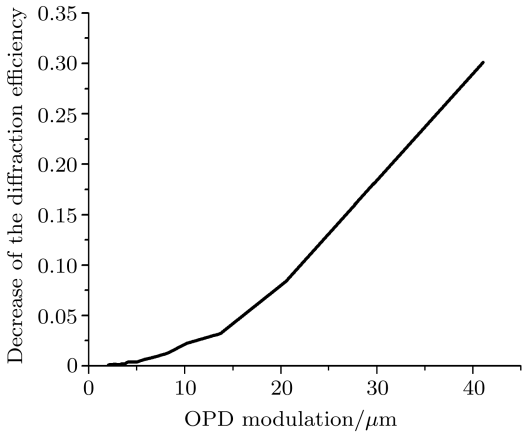


Fig.9. The decrease of the diffraction efficiency as a function of $\mathrm{OPD_L}$, the pixel size is 19 μm.

3.3. Effects of black matrix

The small interval occurred between each pixel is caused by Black Matrix as shown in Fig.10. It also affects the diffraction efficiency of the LC SLM as shown

in Fig.11. It is shown that the diffraction efficiency decreases 6.4%, 8.8%, 9.5% and 9.7% respectively for 4, 8, 16 and 32 levels while pixel interval is 1 μm and pixel pitch is 20 μm. Consequently, the effect magnitude of the diffraction efficiency increases for larger number quantified levels and the maximum decrease of the diffraction efficiency is about 10%.

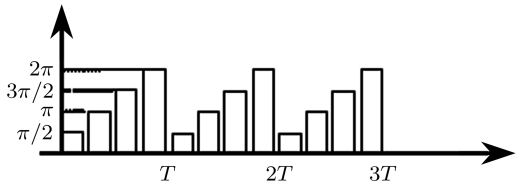


Fig.10. Fresnel phase lens quantified by the pixel with Black Matrix.

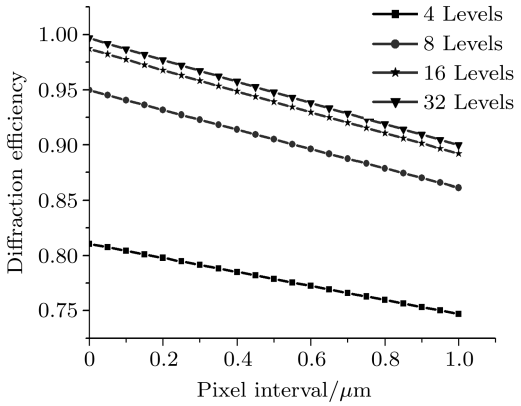


Fig.11. The diffraction efficiency as functions of pixel interval for different quantified level.

4. Discussion

The LC SLM is very suitable for wavefront correction in adaptive optics systems. It is always used to detect and observe the weak object. Consequently, it must realize the correction of the wavefront with high precision and high diffraction efficiency. Ordinarily, if PV is better than $\lambda/10$, a clear image can be obtained. For the LC SLM with 1024×768 pixels and 19 μm pixel size, the maximum $\mathrm{OPD_L}$ is 41 μm for paraboloid wavefront with PV accuracy better than $\lambda/10$. The wavefront distortion of the adaptive optics systems caused by the air turbulence is several microns ordinarily (except for the tilt aberration). Consequently, the LC SLM can realize the high accuracy correction for the air turbulence. Simultaneously, for correcting 10 μm wavefront distortion, the decrease of the diffraction efficiency is 11% or so. Accordingly, it is feasible to correct the distorted wavefront caused by the air turbulence with high diffraction efficiency. However, if we use it to correct 41 μm wavefront distortion, the diffraction efficiency will decrease 40% or so (it is caused by the mismatch and black matrix).

For aspherical testing, the main demand is that the compensator can produce the wavefront with high precision and the large phase change. If the OPD modulation at the LC SLM is 41 μm and the diameter of tested paraboloid is 1 m, the maximum OPD modulation at the tested paraboloid can be calculated with Eq.(16) and 2733 μm OPD modulation is achieved for $\mathrm{PV} \leq \lambda/10$. It is adequate for optical testing. Specially, if the OPD modulation of tested surface is larger than 2733 μm with the same diameter, one spherical wave have to be used as an incident light of the LC SLM to acquire larger phase change. So, the LC SLM is feasible to be used as a compensator in optical testing.

5. Conclusions

Pixel effects on the diffraction efficiency and the phase of the wavefront are analysed with the diffractive theory. A LC SLM with 2 cm×1.5 cm area, 1024×768 pixels, and 19 μm pixel size is used.

First, the wavefront deviation caused by the pixel size is discussed. The calculated results show that the quantified level is at least 4 at the edge of the wavefront in order to achieve the PV accuracy better than $\lambda/10$ ($\lambda = 632.8$ nm). The eccentricity e has almost no effect on the wavefront. It indicates that the PV correction accuracy may be better than $\lambda/10$ while the $\mathrm{OPD_L}$ is less than 41 μm.

The effects caused by mismatch and black matrix on the diffraction efficiency are also considered. If only the mismatch is considered, the decrease of the diffraction efficiency is 1% while each period of the Fresnel lens occupies not less than 7 pixels and the diffraction efficiency reduces by 30% on the condition that the LC SLM is used to correct or produce 41 μm OPD. Due to the effect of the black matrix, the diffraction efficiency has more reduction while the quantified level increases and the maximum decrease of the diffraction efficiency is 10% or so.

Finally, we investigate the feasibility for the LC SLM in the applications of optical testing and wavefront correction. As the wavefront distortion of the adaptive optics systems caused by the air turbulence

is several microns, the decrease of the diffraction efficiency is less than 11% and the correction precision is better than $\lambda/10$ for wavefront correction. Consequently, the LC SLM can be used as a wavefront corrector in adaptive optics system. The calculated results and the discussions show that it can satisfy the demand of optical testing.

Although we just investigate the feasibility for wavefront correction and optical testing, these results can also be used to evaluate the applications of the LC SLM in beam steering, computer generated holograph, and spatial filter, etc.

References

[1] Liu X M, Liu L R and Bai L H 2006 *Chin. Phys.* **15** 708

[2] Lü R B, Xu K S, Zhang S Y, Gu X, Xing Z J, Deng H H, Gu G H, Xiao Z D and Lu Z H 1999 *Acta Phys. Sin.* **8** 670 (in Chinese)

[3] Hu L F, Xuan L, Liu Y J, Cao Z L, Li D Y and Mu Q Q 2004 *Opt. Express* **12** 6403

[4] Cao Z L, Xuan L, Hu L F, Liu Y J, Mu Q Q and Li D Y 2005 *Opt. Express* **13** 1059

[5] Cao Z L, Xuan L, Hu L F, Liu Y J and Mu Q Q 2005 *Opt. Express* **13** 5186

[6] Dayton David, Browne Steve and Gonglewski John 2005 *SPIE* **5894** 58940M-1

[7] Wang X H, Wang B, John Pouch, Felix Miranda, Anderson James E and Bos Philip J 2004 *Opt. Eng.* **43** 2769

[8] Ge A M, Sui Z and Xu K S 2003 *Acta Phys. Sin.* **52** 2481 (in Chinese)

[9] Wei H Z, Zhang Z G, Chen S H, Chai L and Wang Q Y 2004 *Acta Phys. Sin.* **53** 1391 (in Chinese)

[10] Amako J and Sonehara T 1991 *Appl. Opt.* **30** 4622

[11] Hu L F 2005 *Chin. J. Liquid Cryst. Displays* **20** 93 (in Chinese)

[12] J A, Jordan J, Hirsch P M, Lesem L B and Van Rooy D L 1970 *App. Opt.* **9** 1883

[13] Moreno Lgnacio, Lemmi Claudio, Márquez Andrés, Campos Juan and Yzuel Maria J 2004 *Appl. Opt.* **43** 6278

[14] Laude Vincent 1998 *Opt. Commun.* **153** 134

[15] CarcoléE, Campos J and Bosch S 1994 *Appl. Opt.* **33** 162

[16] Golub M A, Sisakjan I N and Soifer V A 1990 *SPIE* **1334** 188

[17] Ferstl Margit, Kuhlow Berndt and Pawlowski Edgar 1994 *Opt. Eng.* **33** 1229

[18] Li H J, Lu Z W, Liao J H, and Weng Z C 2000 *Acta Photon. Sin.* **29** 559 (in Chinese)